Dalton Transactions

Accepted Manuscript

This is an *Accepted Manuscript*, which has been through the Royal Society of Chemistry peer review process and has been accepted for publication.

Accepted Manuscripts are published online shortly after acceptance, before technical editing, formatting and proof reading. Using this free service, authors can make their results available to the community, in citable form, before we publish the edited article. We will replace this *Accepted Manuscript* with the edited and formatted *Advance Article* as soon as it is available.

You can find more information about *Accepted Manuscripts* in the Information for Authors.

Please note that technical editing may introduce minor changes to the text and/or graphics, which may alter content. The journal's standard Terms & Conditions and the Ethical guidelines still apply. In no event shall the Royal Society of Chemistry be held responsible for any errors or omissions in this *Accepted Manuscript* or any consequences arising from the use of any information it contains.

ROYAL SOCIETY OF CHEMISTRY

www.rsc.org/dalton

Journal Name

RSCPublishing

COMMUNICATION

A nickel complex with a biscarbene pincer-type ligand shows high electrocatalytic reduction of CO_2 over H_2O

Cite this: DOI: 10.1039/x0xx00000x

Meili Sheng,[a] Nan Jiang,[a] Samantha Gustafson,[b] Bo You,[a] Daniel H. Ess,[*b] and Yujie Sun[*a]

Received 00th January 2012,
Accepted 00th January 2012

DOI: 10.1039/x0xx00000x

www.rsc.org/

We report a planar nickel complex coordinated with a pincer-type carbene-pyridine-carbene ligand which exhibits high selectivity for electrocatalytic CO_2 reduction in the presence of H_2O.

Catalytic conversion of CO_2 to fuels and value-added fine chemicals has the potential to offset some fossil fuel combustion.[1] To realize a large-scale deployment of CO_2 reduction, it is critical to develop low-cost catalysts that selectively reduce CO_2 over competing H_2 evolution reaction (HER). Heterogeneous transition-metal catalysts, [2] such as Cu, Ag, Au, Sn, and Pd-based nanocomposites,[3,4] have emerged as promising CO_2 reduction catalysts, but the lack of molecular-level mechanistic understanding of catalytic active sites impedes further development. Discrete molecular/homogeneous catalysts offer the advantage of direct catalytic activity tuning through ligand design and direct catalyst performance testing through spectroscopic detection.

The two-electron/two-proton reduction of CO_2 to CO is an appealing process because CO can be directly utilized as a fuel or commodity chemical in mature industrial processes.[1] At pH 7 the thermodynamic potential of CO_2 reduction to CO is –0.53 V vs standard hydrogen electrode (SHE)[5] while HER requires a less negative potential, –0.413 V vs SHE. Therefore, it is imperative to develop CO_2 reduction catalysts with a particularly high selectivity over HER in the presence of H_2O or other proton sources that may divert reducing power and lower Faradaic efficiency. Many molecular CO_2 reduction catalysts utilize ligands of porphyrins,[6] phthalocyanines,[7] polypyridines,[8] and phosphines,[9] most of which require sophisticated synthetic routes and/or are moisture/air sensitive. Nearly two decades ago, Sauvage et al. reported nickel complexes bearing N_4-macrocycles (cyclam) that exhibited remarkable high selectivity for CO_2 reduction over HER.[10] Since Sauvage's seminal work, only a limited number of nickel catalysts have been reported showing comparable or better performance than the $[Ni(cyclam)]^{2+}$ system.[11]

Following the design principle of $[Ni(cyclam)]^{2+}$, a number of planar tetradentate ligands have been employed in the development of nickel-based catalysts for CO_2 reduction.[12] In contrast, we reason that a tridentate pincer-type ligand would also support Ni^{2+} in a pseudo square planar geometry if the fourth site can be occupied by a labile solvent molecule. Such a strategy not only allows the accessibility of the apical site of the nickel center towards CO_2, but also might lead to an exchange of the bound solvent molecule and CO_2 at one of the equatorial sites, enriching the interaction mode of CO_2 with the catalyst. Herein, we report the synthesis, experimental and computational characterization, and evaluation of a nickel complex coordinated with a pyridyl-biscarbene pincer-type ligand which shows high selectivity for electrocatalytic CO_2 reduction over HER.

The nickel [(CNC)NiBr]Br complex with a pincer-type biscarbene ligand ($CNCBr_2$, Fig. 1) was previously reported as a catalyst for Heck and Suzuki coupling reactions.[13] To avoid the influence of redox active Br^- and Br_2, we treated $CNCBr_2$ with AgOTf (OTf = trifluoromethanesulfonate) to obtain $CNC(OTf)_2$. Subsequent metalation of $CNC(OTf)_2$ with nickel triflate in CH_3CN formed $[(CNC)Ni(NCCH_3)](OTf)_2$ (CNC-Ni, Fig. 1). Slow vapor diffusion

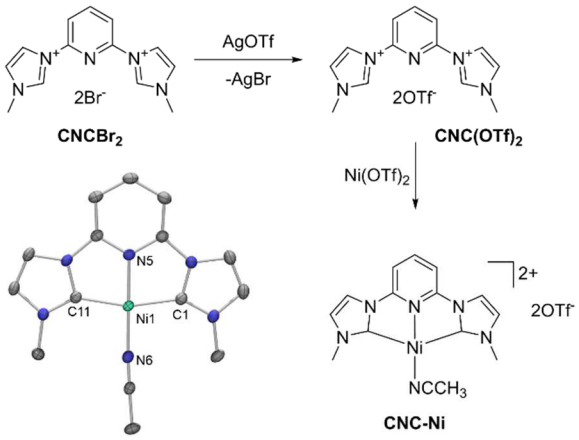

Fig.1 Synthetic scheme of CNC-Ni and its crystal structure with thermal ellipsoids drawn at the 50% probability level. Two triflate counter ions and hydrogen atoms are omitted for clarity. Selected bond lengths (Å) and angles (deg): Ni1–N6 = 1.8397(13), Ni1–N5 = 1.8514(13), Ni1–C11 = 1.9120(15), Ni1–C1 = 1.9207(16); N6–Ni1–N5 = 176.59(6), N6–Ni1–C11 = 98.79(6), N5–Ni1–C11 = 81.55(6), N6–Ni1–C1 = 98.02(6), N5–Ni1–C1 = 81.73(6), C11–Ni1–C1 = 163.15(7).

Dalton Transactions Accepted Manuscript

of diethyl ether into the concentrated CH_3CN solution of CNC-Ni produced light yellow crystalline needles. The structure of CNC-Ni was obtained by single crystal X-ray diffraction (Fig. 1). As expected, the diamagnetic Ni^{II} CNC-Ni complex is in a pseudo square planar geometry. Similar to the crystal structure of [(CNC)NiBr]Br,[13] the Ni1-N5 and Ni1-N6 distances of CNC-Ni fall in the region of 1.83–1.85 Å, while Ni-C1 and Ni-C11 bonds are within 1.91–1.92 Å. The N5-Ni1-N5 angle (176.6°) slightly deviates from 180° angle expected for a square planar geometry. Geometric constraint of the pyridyl linker between the two imidazole rings results in a C1-Ni1-C11 angle of 163.2°. Overall, the tridentate pincer-type ligand combined with a CH_3CN occupying the fourth planar coordination site provides a catalyst with the possibility to interact with CO_2 at either the apical site or the equatorial site if CH_3CN dissociates after catalyst reduction.

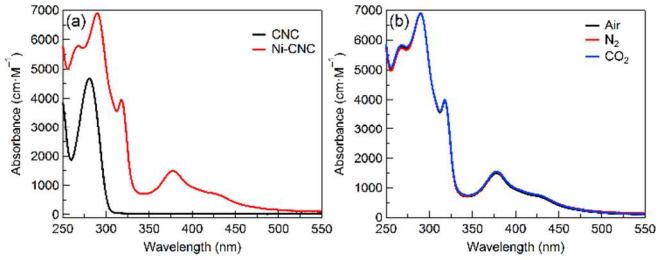

Fig.2 (a) UV-visible absorbance of free ligand (black) and CNC-Ni (red) in acetonitrile under air. (b) Comparison of the UV-visible absorbance spectra of CNC-Ni in acetonitrile under air (black), N_2 (red), and CO_2 (blue).

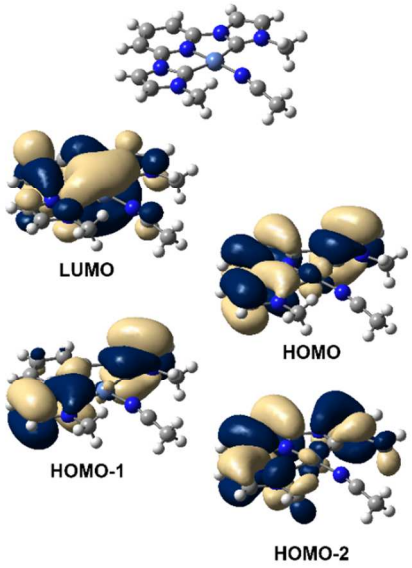

Fig. 3 M06 molecuar orbitals corresponding to TD-DFT excitations for CNC-Ni.

UV-visible absorbance spectra of CNC-Ni and the free ligand $CNC(OTf)_2$ in CH_3CN are compared in Fig. 2(a). The absorbance of $CNC(OTf)_2$ only features a strong peak at 281 nm (4,681 M^{-1} cm^{-1}) in the UV region, potentially due to a π-to-π* transition. To model this and other absorbances, we carried out (U)M06/LANL2TZ(f)(6-311+G(2d,p))//M06/LANL2DZ(6-31G(d,p)) TD-DFT calculations in Gaussian 09 (see SI for details).[14] With the implicit SMD[15] solvent model for CH_3CN the major excitation calculated above 250 nm is at 276 nm. Indeed, this excitation is principally a π-to-π* (HOMO to LUMO) transition.

The pale yellow solution of CNC-Ni shows a prominent peak at 290 nm (6,899 M^{-1} cm^{-1}) with two shoulder peaks at 268 nm (5,782 M^{-1} cm^{-1}) and 318 nm (3,967 M^{-1} cm^{-1}). In addition, there exists another broad feature with a maximum at 377 nm (1,501 M^{-1} cm^{-1}). The major calculated excitation at 284 nm corresponds to ligand-to-metal charge transfer (LMCT) from HOMO-2 to LUMO (Fig. 3). There is a TD-DFT excitation at 307 nm that corresponds to a weak HOMO-1 to LUMO transition. The TD-DFT calculations also show a very weak transition at 361 nm, which can be attributed to a HOMO-LUMO excitation that results in LMCT.

In order to test whether CO_2 is able to bind CNC-Ni, UV-visible absorbance was also measured under different atmospheres. As shown in Fig. 2b, the perfect overlap of the absorbance spectra of CNC-Ni under air, N_2, and CO_2 excludes the possibility of CO_2 binding to CNC-Ni prior to electrochemical reduction. Our DFT calculations also suggest that both CO_2 and CO_2/H_2O apical coordination to CNC-Ni are not stable. Additionally, the coordination energy of CH_3CN to CNC-Ni is ~25 kcal/mol and therefore at ambient temperature CO_2 is also unlikely to interchange with CH_3CN.

We next assessed the capability of CNC-Ni as an electrocatalyst for CO_2 reduction in CH_3CN. Fig. 4 displays the cyclic voltammogram of CNC-Ni under N_2. Two irreversible reduction peaks were observed at –1.19 and –1.38 V vs. $Fc^{+/0}$ ($Fc^{+/0}$ = ferrocenium/ferrocene redox couple; unless otherwise noted, all the potentials reported are versus $Fc^{+/0}$.). Scanning towards further negative potential reveals a third irreversible peak at –1.77 V. The blank glassy carbon is redox silent in this potential region. Plotting the peak currents at these potentials versus the square root of scan rates leads to a linear relationship for each redox process (Fig. S1 in the SI), confirming the molecular nature of CNC-Ni dissolved in the bulk electrolyte and no absorbed species on the electrode surface was contributing to the measured electrochemical signal. The free ligand $CNC(OTf)_2$ only exhibits one irreversible peak at –1.79 V prior to –2 V under the same condition (Fig. S2a). Because of the similarity between the third reduction peak (–1.77 V) of CNC-Ni and the reduction peak (–1.79 V) of $CNC(OTf)_2$, the former is attributed to a ligand-based redox process.

The calculated $Ni^{II/I}$ absolute reduction free energy of CNC-Ni is –87.6 kcal/mol. Relative to the experimental $Fc^{+/0}$ couple value of –114.8 kcal/mol (–4.98 V) in CH_3CN, this results in a calculated $Ni^{II/I}$ value of –1.19 V that is identical to experiment (see SI for prediction of alternative density functionals). A plot of the α-spin density

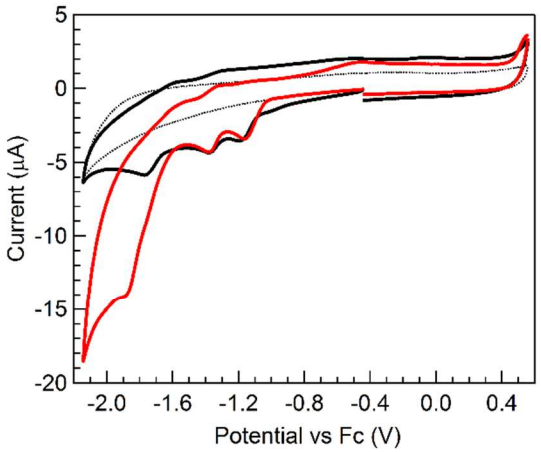

Fig. 4 Cyclic voltammograms of blank under N_2 (dotted black) and CNC-Ni under N_2 (solid black) and CO_2 (solid red) in CH_3CN with 0.1

Dalton Transactions Accepted Manuscript

This journal is © The Royal Society of Chemistry 2012

M Bu_4PF_6 as the supporting electrolyte (scan rate: 100 mV/s).

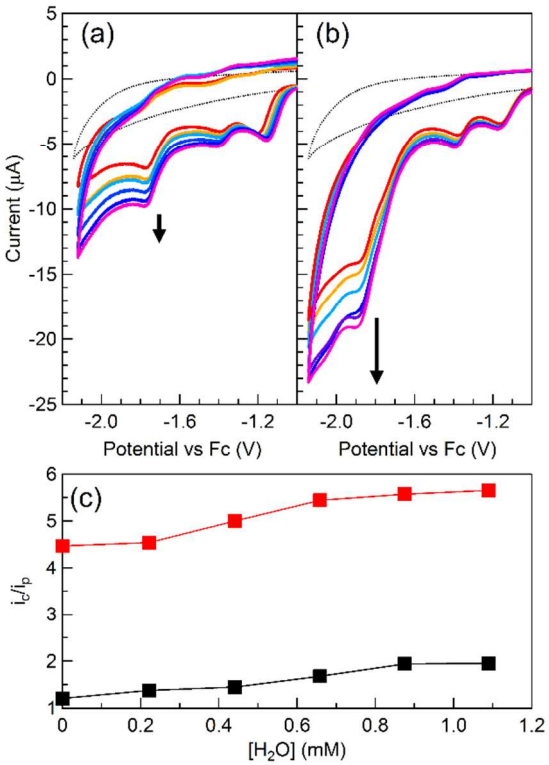

Fig. 5 Cyclic voltammograms of CNC-Ni under (a) N_2 and (b) CO_2 with increasing addition of H_2O from 0 to 1.1 mM. (c) The comparison of i_c/i_p versus the concentration of H_2O ([H_2O]) in CH_3CN for CNC-Ni under N_2 (black) and CO_2 (red). i_c is the cathodic current at −1.77 V (N_2) or −1.85 V (CO_2); while i_p is the cathodic current of the first reduction peak in each cyclic voltrammogram. Background current from the blank glassy carbon electrode was subtracted in calculating i_c/i_p.

polarization for $[(CNC)Ni^{I}(NCCH_3)]^+$ suggests that the excess spin density upon reduction of CNC-Ni occurs at the Ni metal center, but is also partially delocalized onto the CNC ligand framework.

In CO_2-saturated CH_3CN, the first two reduction peaks of CNC-Ni remained at the same potentials (Fig. 4), implying the parent nickel complex did not interact with CO_2 substantially which is consistent with the UV-vis absorbance results. However, a current enhancement was observed prior to the third reduction peak, showing an onset at −1.55 V. Such a dramatic current increase is indicative of electrocatalytic CO_2 reduction. It should be noted that the catalytic onset is less negative compared to that of Chang's nickel catalyst for CO_2 reduction (beyond −1.6 V) under a similar condition. Furthermore, the intrinsic turnover frequency of CNC-Ni calculated from its cyclic voltammogram in Fig. 4 is 90 s^{-1} (see ESI for details) higher than those (4 – 6 h^{-1}) of the reported nickel catalysts coordinated with tetradentate pyridyl-carbene ligands. The $CNC(OTf)_2$ free ligand exhibited negligible current enhancement under the same condition (Fig. S2a), demonstrating the observed CO_2 reduction was due to the intact CNC-Ni.

Upon addition of water, further enhancement of catalytic current of CNC-Ni was observed under CO_2 (Fig 5b). In contrast, as plotted in Fig. 5a and c, under N_2 CNC-Ni showed a negligible cathodic current enhancement upon addition of water, suggesting CNC-Ni was not effective in water reduction to produce H_2. Further increasing water concentration beyond 0.8 mM did not lead to increased catalytic current under either N_2 or CO_2. We also evaluated the influence of D_2O addition as shown in Fig. S3, which did not exhibit any substantial difference from those upon addition of H_2O under CO_2. Although H_2O facilitated CO_2 reduction, the lack of a hydrogen isotope effect excludes proton transfer as a rate-limiting step. It should be noted that the addition of H_2O did not affect the reduction feature of the free ligand $CNC(OTf)_2$ under either CO_2 or N_2 (Fig. S2b), demonstrating it was not effective in activating either CO_2 or H_2O.

Long-term controlled potential electrolysis of CNC-Ni at −1.773 V for two hours in CO_2-saturated CH_3CN with 0.4 mM H_2O was conducted (Fig. S4). Only CO was produced as the major product and no detectable H_2 was obtained via gas chromatography (Fig. S5), further confirming the high selectivity of CNC-Ni for electrocatalytic reduction of CO_2 over H_2O. Overall, these results demonstrated that CNC-Ni acts as a highly selective electrocatalyst for CO_2 reduction over HER in the presence of a proton source and its catalytic rate is not limited by proton transfer.

Based on these experimental and computational results, a possible mechanism of CO_2 reduction catalysed by CNC-Ni proceeds via two consecutive one-electron reductions from Ni^{II} to Ni^{0}, where CH_3CN may dissociate and allow coordination of CO_2. Subsequent proton facilitated steps result in the formation of CO. The exact catalytic intermediates and mechanistic steps are under further investigation.

In summary, we have presented a nickel complex supported by a pincer-type carbene-pyridyl-carbene ligand exhibiting high selectivity for the electrocatalytic reduction of CO_2 over H_2O. The facile synthesis of the platform will allow us to modify the electronic substituents of the ligand, investigate the catalytic selectivity for reducing CO_2 employing other first-row transition metals, and couple to chromophores for photocatalytic CO_2 reduction, which are our current pursuits.

Y.S. thanks Utah State University for support of this work. D.H.E and Y.S. thank the State of Utah via the Principle Energy Issues Program for financial support. D.H.E also thanks BYU and the Fulton Supercomputing Lab. N.J. acknowledges the Governor's Energy Leadership Scholars Grant program of the State of Utah.

Notes and references

[a]Department of Chemistry and Biochemistry, Utah State University, Logan, Utah 84322, USA. E-mail: yujie.sun@usu.edu; Tel: +1-435-797-7608

[b]Department of Chemistry and Biochemistry, Brigham Young University, Provo, Utah 84602, USA. E-mail: dhe@byu.edu; Tel: +1-801-422-9164.

Electronic Supplementary Information (ESI) available: Experimental and computational details. See DOI: 10.1039/c000000x/

1 (a) M. Mikkelsen, M. Jorgensen and F. C. Krebs, *Energy Environ. Sci.*, 2010, **3**, 43-81; (b) A. M. Appel, J. E. Bercaw, A. B. Bocarsly, H. Dobbek, D. L. DuBois, M. Dupuis, J. G. Ferry, E. Fujita, R. Hille, P. J. A. Kenis, C. A. Kerfeld, R. H. Morris, C. H. F. Peden, A. R. Portis, S. W. Ragsdale, T. B. Rauchfuss, J. N. H. Reek, L. C. Seefeldt, R. K. Thauer and G. L. Waldrop, *Chem. Rev.*, 2013, **113**, 6621-6658.

2 Q. Lu, J. Rosen and F. Jiao, *ChemCatChem*, 2015, **7**, 38-47.

3 (a) C. W. Li and M. W. Kanan, *J. Am. Chem. Soc.*, 2012, **134**, 7231-7234; (b) Y. Chen and M. W. Kanan, *J. Am. Chem. Soc.*, 2012, **134**, 1986-1989; (c) C. H. Lee and M. W. Kanan, *ACS Catal.*, 2014, **5**, 465-469; (d) X. Min, Y. Chen and M. W. Kanan, *Phys. Chem. Chem. Phys.*, 2014, **16**, 13601-13604; (e)X. Feng, K. Jiang, S. Fan and M. W. Kanan, *J. Am. Chem. Soc.*, 2015, **137**, 4606-4609.

4 Q. Lu, J. Rosen, Y. Zhou, G. S. Hutchings, Y. C. Kimmel, J. G. Chen and F. Jiao, *Nat. Commun.*, 2014, **5**, 3242.

5 A. J. Morris, G. J. Meyer and E. Fujita, *Acc. Chem. Res.*, 2009, **42**, 1983-1994.

Dalton Transactions Accepted Manuscript

6 (a) I. Bhugun, D. Lexa and J.-M. Savéant, *J. Am. Chem. Soc.*, 1996, **118**, 1769-1776; (b) J. Grodkowski, P. Neta, E. Fujita, A. Mahammed, L. Simkhovich and Z. Gross, *J. Phys. Chem. A*, 2002, **106**, 4772-4778; (c) C. Costentin, S. Drouet, M. Robert and J.-M. Savéant, *Science*, 2012, **338**, 90-94; (d) C. Costentin, G. Passard, M. Robert and J.-M. Savéant, *Proc. Natl. Acad. Sci. USA*, 2014, **111**, 14990-14994.

7 (a) S. Meshitsuka, M. Ichikawa and K. Tamaru, *J. Chem. Soc., Chem. Commun.*, 1974, 158-159; (b) C. M. Lieber and N. S. Lewis, *J. Am. Chem. Soc.*, 1984, **106**, 5033-5034; (c) S. Kapusta and N. Hackerman, *J. Electrochem. Soc.*, 1984, **131**, 1511-1514.

8 (a) H. Ishida, K. Tanaka and T. Tanaka, *Organometallics*, 1987, **6**, 181-186; (b) C. M. Bolinger, N. Story, B. P. Sullivan and T. J. Meyer, *Inorg. Chem.*, 1988, **27**, 4582-4587; (c) C. Arana, S. Yan, M. Keshavarz-K, K. T. Potts and H. D. Abruna, *Inorg. Chem.*, 1992, **31**, 3680-3682; (d) Z. Chen, C. Chen, D. R. Weinberg, P. Kang, J. J. Concepcion, D. P. Harrison, M. S. Brookhart and T. J. Meyer, *Chem. Commun.*, 2011, **47**, 12607-12609; (e) M. Bourrez, F. Molton, S. Chardon-Noblat and A. Deronzier, *Angew. Chem. Int. Ed.*, 2011, **50**, 9903-9906; (f) W.-H. Wang, J. F. Hull, J. T. Muckerman, E. Fujita and Y. Himeda, *Energy. Environ. Sci.*, 2012, **5**, 7923-7926; (g) Z. Chen, P. Kang, M.-T. Zhang and T. J. Meyer, *Chem. Commun.*, 2014, **50**, 335-337.

9 (a) E. Simón-Manso and C. P. Kubiak, *Organometallics*, 2005, **24**, 96-102; (b) M. Rakowski Dubois and D. L. Dubois, *Acc. Chem. Res.*, 2009, **42**, 1974-1982; (c) P. Kang, C. Cheng, Z. Chen, C. K. Schauer, T. J. Meyer and M. Brookhart, *J. Am. Chem. Soc.*, 2012, **134**, 5500-5503.

10 (a) M. Beley, J.-P. Collin, R. Ruppert and J.-P. Sauvage, *J. Chem. Soc., Chem. Commun.*, 1984, 1315-1316; (b) M. Beley, J. P. Collin, R. Ruppert and J. P. Sauvage, *J. Am. Chem. Soc.*, 1986, **108**, 7461-7467; (c) J. D. Froehlich and C. P. Kubiak, *Inorg. Chem.*, 2012, **51**, 3932–3934.

11 (a) J. P. Collin, A. Jouaiti and J. P. Sauvage, *Inorg. Chem.*, 1988, **27**, 1986-1990; (b) E. Fujita, J. Haff, R. Sanzenbacher and H. Elias, *Inorg. Chem.*, 1994, **33**, 4627-4628; (c) J. D. Froehlich and C. P. Kubiak, *Inorg. Chem.*, 2012, **51**, 3932-3934; (d) J. Schneider, H. Jia, K. Kobiro, D. E. Cabelli, J. T. Muckerman and E. Fujita, *Energy. Environ. Sci.*, 2012, **5**, 9502-9510.

12 (a) V. S. Thoi and C. J. Chang, *Chem. Commun.*, 2011, **47**, 6578-6580; (b) V. S. Thoi, N. Kornienko, C. G. Margarit, P. Yang and C. J. Chang, *J. Am. Chem. Soc.*, 2013, **135**, 14413-14424.

13 K. Inamoto, J.-i. Kuroda, K. Hiroya, Y. Noda, M. Watanabe and T. Sakamoto, *Organometallics*, 2006, **25**, 3095-3098.

14 (a) M. J. Frisch, et al. *Gaussian* 09, revision A.02 and B.01; Gaussian, Inc., Wallingford, CT 2009; (b) Y. Zhao and D. T. Truhlar, *Theor. Chem. Acc.*, 2008, **120**, 215-241; (c) Y. Zhao and D. T. Truhlar, *Acc. Chem. Res.*, 2008, **41**, 157-167; (d) P. J. Hay and W. R. Wadt, *J. Chem. Phys.*, 1985, **82**, 270-283; (e) P. J. Hay and W. R. Wadt, *J. Chem. Phys.*, 1985, **82**, 284-298; (f) P. J. Hay and W. R. Wadt, *J. Chem. Phys.*, 1985, **82**, 299-310.

15 A. V. Marenich, C. J. Cramer and D. G. Truhlar, *J. Phys. Chem. B*, 2009, **113**, 6378-6396.

Dalton Transactions Accepted Manuscript

 This journal is © The Royal Society of Chemistry 2012

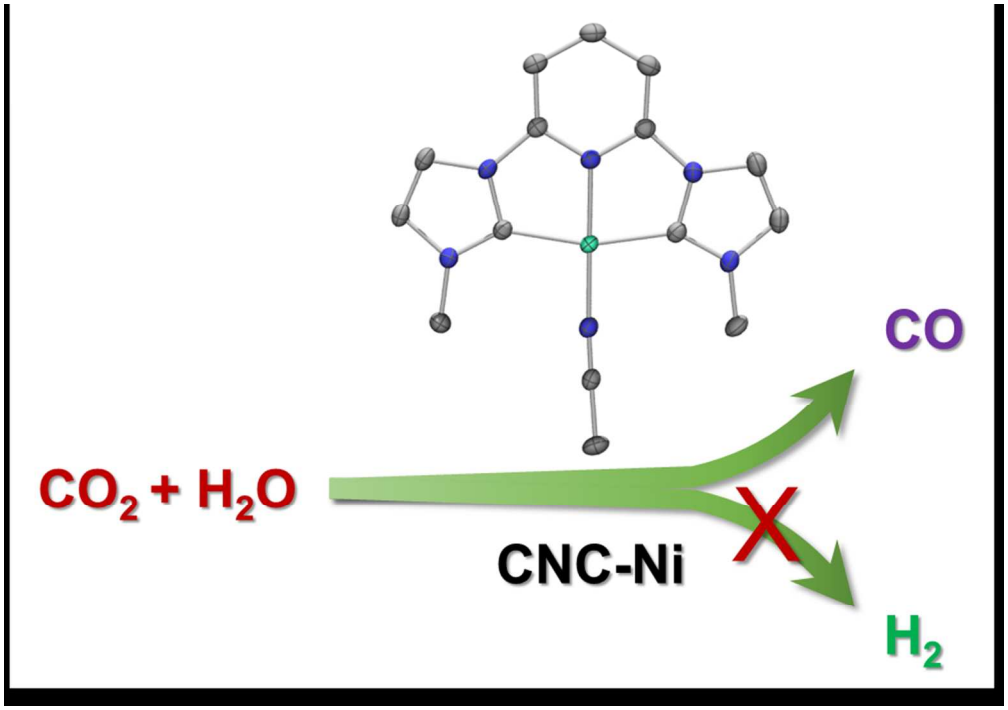

169x118mm (150 x 150 DPI)

Dalton Transactions Accepted Manuscript